JOURNAL OF MATERIALS SCIENCE **34** (1999) 5285–5291

Photoelectrochemical behaviour of CdS "Q-state" semiconductor particles in 10,12-nonacosadiynoic acid polymer langmuir-blodgett films

H. S. MANSUR*, W. L. VASCONCELOS
Metallurgical and Materials Eng. Dep., Universidade Federal de Minas Gerais, Brazil
E-mail: hmansur@demet.ufmg.br

F. GRIESER
University of Melbourne—CSIRO, Division of Chemicals and Polymers, Private Bag 10, Rosebank MDC, Clayton, Victoria 3169, Australia

F. CARUSO
Max-Planck-Institute of Colloids and Interfaces, Rudower Chaussee 5, D-12489 Berlin, Germany

CdS "Q-state" semiconductor particles from 2 to 10 nm diameter were nucleated and grown in 10,12-nonacosadiynoic acid (NCDA) polymer Langmuir-Blodgett (LB) films deposited on ITO plates. The polymerization process through exposure to UV-Visible light resulted in formation of the "blue form" followed by the final "red form" after 60 min. X-ray photoelectron spectroscopy (XPS) measurements confirmed the deposition of the NCDA cadmium salt and the formation of the CdS particles after exposure to $H_2S_{(g)}$ in the LB matrix. A study of the photoelectrochemical behaviour of these systems was conducted through polarisation current-voltage (I-V) curves in the range of 0 to −1000 mV (Standard Calomel Electrode-SCE). An average open-circuit voltage (V_{OC}) from −600 to −700 mV values was observed for photoelectrochemical (PEC) cells constructed for the undoped NCDA polymer LB film with 10 nm diameter CdS particles. The I_2-doped NCDA polymer film presented an increase in the conductivity compared with the undoped film but with a deterioration of stability of the PEC system.

1. Introduction

Over the past few years we have been working on the formation of cadmium chalcogenides nanoparticles in LB films [1–9]. We have deposited multilayers of Cd-[organic chain] onto either silica or mica plates and then exposing these films to a particular chalcogenide gas ($H_2S_{(g)}$, $H_2Se_{(g)}$, $H_2Te_{(g)}$). Using a quartz crystal microbalance we have shown the reaction of the gas with the metal ion in the film is quantitative and that the rate of reaction is dependent on the film thickness [1]. We have also found that the semiconductor material formed in the film shows size quantization effects, much like what is found when ultrasmall semiconductor particles are formed in other organized media. We have verified that the metal chalcogenides formed in the LB film have a spheroidal morphology [3–4].

The LB organic matrix works as constraining agent for particle growth, "capping" the semiconductor particles. Therefore, it plays an important role in determining the size of the particles generated in the film matrix. It becomes obvious that other metal ions can be incorporated into the film by simply immersing the film in an aqueous solution possessing a suitable "binding" ion. We have made use of this feature of the LB film in the presence of cadmium sulfide particles, and have found that exposing this film to H_2S gas after it had been immersed in a $CdCl_2$ solution, results in an increase in the size of the particles in the host LB film [2].

More recently we have been examining the photoelectrochemical properties of these semiconductor particle-LB films with the aim of understanding some of the fundamental photochemical properties of quantum sized metal chalcogenides, and as a method of gaining information on the spatial distribution of the particles formed in the films. The present study is an extension of that work and we report on the photoelectrochemical behaviour of the semiconductor/liquid junction based on CdS "Q-State" size particles supported in conductive polymeric LB films.

2. Experimental

2.1. Materials

Cadmium chloride and potassium hydrogen carbonate were analytical grade reagents from Fluka Chemika and

---

*Author to whom all correspondence should be addressed. Escola de Engenharia, Universidade Federal de Minas Gerais, Rua Espirito Santo, 35/2° Andar, CEP 30160-030, BH, MG, Brazil.

0022–2461

were used without further purification. Chloroform and *n*-hexane (spectroscopic UV grade from Ajax Chemicals) were used to prepare monolayer spreading solutions and for cleaning the Langmuir trough before use.

The polymerizable diluent 10,12-nonacosadiynoic acid (NCDA or 16-8 diacetylene) was purchased from Tokyo Kasei. NCDA was purified by recrystallization from diethyl ether (Ajax, AR grade) immediately before use to remove any polymer residue.

Optically transparent electrodes (OTE), obtained from Hoya Corp. Japan, were cut from 1.0 × 100 × 100 mm indium-tin oxide (ITO) coated glass with a conductive layer thickness of 200 nm and an electrical resistivity of 1 Ω/mm.

The ITO plates were cleaned and made hydrophilic by soaking in a hot aqueous solution containing 27% (w/v) of H_2O_2 and 2% (w/v) of NH_4OH, for 30 min. The plates were then rinsed with copious amounts of Milli-Q water ($\kappa < 1.0 \times 10^{-4}$ S m^{-1}) and stored immersed in Milli-Q water until required for LB film deposition.

Hydrogen sulfide, from CIG, was used as supplied. Iodine resublimated from Unilab was used without further purification.

2.2. Surface pressure-area measurements

Surface pressure-area (π-A) measurements were conducted on a 708.0 × 138.7 mm poly(tetrafluoroethylene) (PTFE) coated Langmuir trough, with a PTFE barrier, driven at a compression rate of 1.18 nm^2.mol^{-1}.m^{-1}. All surface pressure-area measurements were made by the Wilhelmy hanging plate method. Experiments were initiated by filling the trough with the appropriate subphase. π-A measurements were performed using Milli-Q water at $pH = 6.0 \pm 0.1$ and 1.0 mM $CdCl_2$ aqueous solution at $pH = 7.0 \pm 0.1$ as subphases. Approximately 10^{17} molecules from 3 mM chloroform solutions mixed to the desired ratio were spread onto the subphase, using a 100 μl SGE syringe. The solvent was then allowed to evaporate for 10 min, after which the monolayer was compressed as desired.

2.3. Langmuir-Blodgett film preparation

The deposition of 10,12-nonacosadiynoic acid (NCDA) Langmuir-Blodgett (LB) multilayer film was conducted at 20 ± 1 °C using a Langmuir-Blodgett trough with dimensions of 550 mm (L) × 164 mm (W) × 22 mm (D).

NCDA monolayers were prepared by spreading 150–200 μl of 3.0×10^{-3} M NCDA solution ($CHCl_3$) onto a 1.0×10^{-3} M $CdCl_2$ (aq) subphase, buffered with 5.0×10^{-5} M $KHCO_3$, at $pH = 7.0 \pm 0.1$. After spreading the monolayer and allowing 30 min for the solvent to evaporate, the monolayer was compressed at a rate of 10 mm/min until the desired surface pressure was attained. Prior to casting, the monolayer was left to equilibrate at the casting pressure for a minimum period of 15 min. The NCDA LB deposition was performed with a vertical dipping speed, for both the upward and the downward strokes, of 5 mm.min^{-1}. During the casting of the monolayers the surface pressure was maintained at 20 ± 1 mNm^{-1}. The NCDA monolayers were allowed to dry in air for 5 min between each dipping stroke before the subsequent layers were deposited. The transfer ratio for the deposition process was obtained by dividing the change of area on the trough surface by the area of the ITO-glass substrate, for each dip. The transfer ratio was found to be 1.0 ± 0.1 on average.

2.4. "Q-state" CdS particle formation

CdS particles were formed by exposing a multilayer NCDA LB film to $H_2S(g)$ in a sealed reaction vessel for a minimum period of 30 min. After each gassing process the samples were immersed in a 1.0×10^{-3} M $CdCl_2$ subphase solution, $pH = 7.0 \pm 0.1$, at 20 ± 1 °C, to allow Cd^{2+}/H^+ ions to exchange and regenerate the NCDA cadmium film [6]. The $CdCl_2$ aqueous solution was gently stirred for a minimum period of 60 min to aid in the exchange reaction.

Each gassing and immersion sequence was monitored via UV-Visible absorbance spectroscopy. Samples with 1, 3 and 5 $H_2S(g)/CdCl_2(aq)$ immersion cycles were prepared on NCDA coated ITO substrates. This method of particle formation produces particles of mean diameter 2, 5 and 10 nm, respectively [2, 3].

2.5. UV-visible absorbance measurements

UV-visible absorbance measurements were conducted using either a Varian CARY 5 spectrophotometer or a Hewlett-Packard 8451A diode array spectrophotometer. The LB coated plates were fitted into a standard 10 mm path length UV-visible absorbance cell [1–3]. The absorbance spectra presented have been corrected for contributions due to the ITO-Glass substrate coated with the LB film.

2.6. X-ray photoelectron spectroscopy (XPS) method

X-ray photoelectron spectroscopy (XPS) measurements were conducted using a Vacuum Generators Escalab V spectrometer with a non-monochromatic 200 W (10 kV, 20 mA) MgK_α source and a hemispherical analyzer operating in fixed analyzer transmission mode. The total pressure in the main vacuum chamber during analysis was typically 2×10^{-7} Pa. Spectra were collected normal to the sample surface. The elements present were identified from survey spectra. High resolution spectra were recorded from individual peaks at 30 eV pass energy with a step width of 0.078 eV/channel. The binding energies for the XPS spectra were referenced to the Cd $3d_{5/2}$ peak at 405.0 eV. The elemental composition of the surface was determined by a first principles approach [10]; atomic number ratios were calculated with integral peak intensities, using a nonlinear Shirley type background, and published values for photoionisation cross-sections [11]. The inelastic mean free path of the photoelectrons was assumed to be proportional to $E^{0.5}$, where E is the kinetic energy [12]. The transmission function of the analyzer had previously been determined to be proportional to $E^{-0.5}$. The random error associated with quantitative elemental analysis was determined to be 5–10% (usually 7–8%).

2.7. I_2 Doping method

NCDA polymer films with CdS "Q-state" particles were placed in a 1000 ml flask reactor with 10 g of fine grinded I_2 crystals on a Petri dish. The reactor was evacuated to reach a minimum pressure of 5 mm Hg. The minimum exposure time to I_2(g) in the reactor was 3 h and an overnight outgassing was performed before running absorbance and the photoelectrochemical measurements.

2.8. LB Film conductivity measurements

LB Film conductivity measurements were conducted using a typical 4-point probe setup (1.0 mm gap distance) connected to a Hewlett-Packard impedance analyser model 4192A, at 1.0 kHz frequency in DC mode.

2.9. Polymerisation

The polymerisation of the NCDA Langmuir-Blodgett films was performed using a 1000 mW UV lamp, model UVG-11 from UVP Inc., at 30 mm vertical distance from the sample, for a minimum period of 60 min. Absorbance spectra were collected at different UV exposures times.

2.10. Photoelectrochemical (PEC) cell

A PEC cell was constructed using a 200 ml Pyrex® vessel, with a platinum counter electrode, and a standard calomel electrode (SCE) as the reference electrode. Fig. 1 shows a schematic drawing of the assembled PEC cell. ITO-Glass substrates coated with multilayer of NCDA polymer, supporting CdS particles, were used as the photoelectrode. Electrical connection to the photoanode was achieved by attaching a wire to the ITO layer with silver epoxy resin. The resin was cured for 24 h at room temperature. The electrolyte used in the PEC cell was 1.0 M Na_2SO_3(aq). The experiments were conducted at 21 ± 1 °C and the pH maintained at 7.25 ± 0.05.

Photoelectrical measurements were conducted in a cabinet which excluded extraneous light. A 150 W xenon lamp was used as the light source. The light from the lamp was passed through a water filter and then a 320 nm cut-off filter before entering the cell. The light intensity incident on the cell was measured by ferri-oxalate actinometry as described in reference

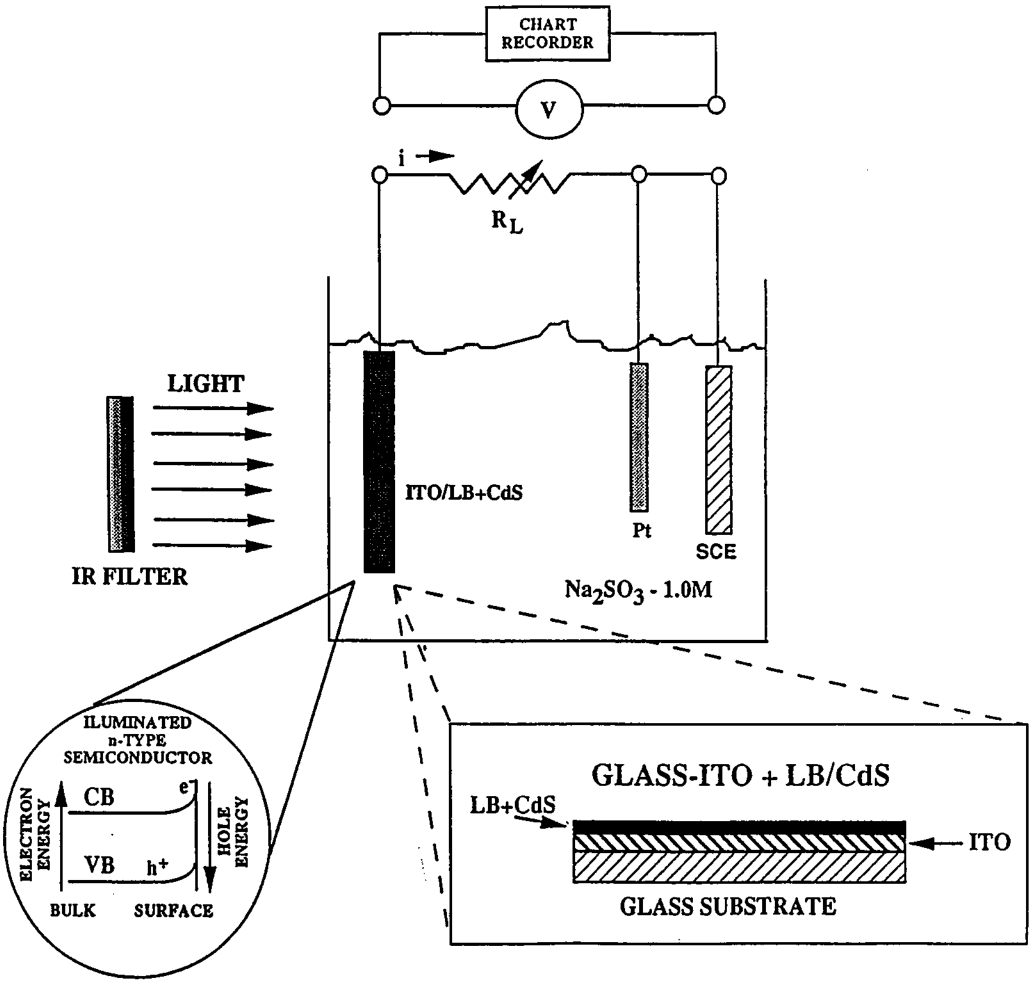

Figure 1 Schematic diagram of the photoelectrochemical cell assembly. Glass/ITO/NCDA-LB+CdS (anode); Pt electrode (cathode); Reference Standard Calomel Electrode (SCE); 1.0 M Na_2SO_3(aq) solution (electrolyte); 150 W xenon lamp ("light source"); external electronic circuit (monitoring I-V signal).

[13]. The average energy flux was $(1.0 \pm 0.1) \times 10^{-4}$ einstein/min, giving 600 ± 50 W/m^2 incident irradiation on the photocell.

The open-circuit voltage (V_{OC}) was obtained as a function of CdS molar concentrations, as well as the mean particle size in the Cd(NCDA)$_2$ LB film. Current-potential (I-V) curves for the PEC cell were obtained through polarisation cycles from 0 to −1000 mV (SCE) using an OE Potentiostat system and a Yokokawa 3025 X-Y recorder.

3. Results

The π-A isotherm for the NCDA (diacetylene 16-8 compound) LB films on pure water and on 1.0×10^{-3} M CdCl$_2$ (aq) subphases are shown in Fig. 2. The area per molecule was found to be of 0.26 nm^2 onto water subphase (Fig. 2a) and 0.22 nm^2 for the CdCl$_2$ (aq) subphase (Fig. 2b). These results are in close agreement with values reported in the literature [14–19]. These π-A isotherms are less condensed than the π-A isotherms for the fully saturated equivalent due to increased steric interactions caused by the linear diacetylene section in the alkyl chain [14, 15].

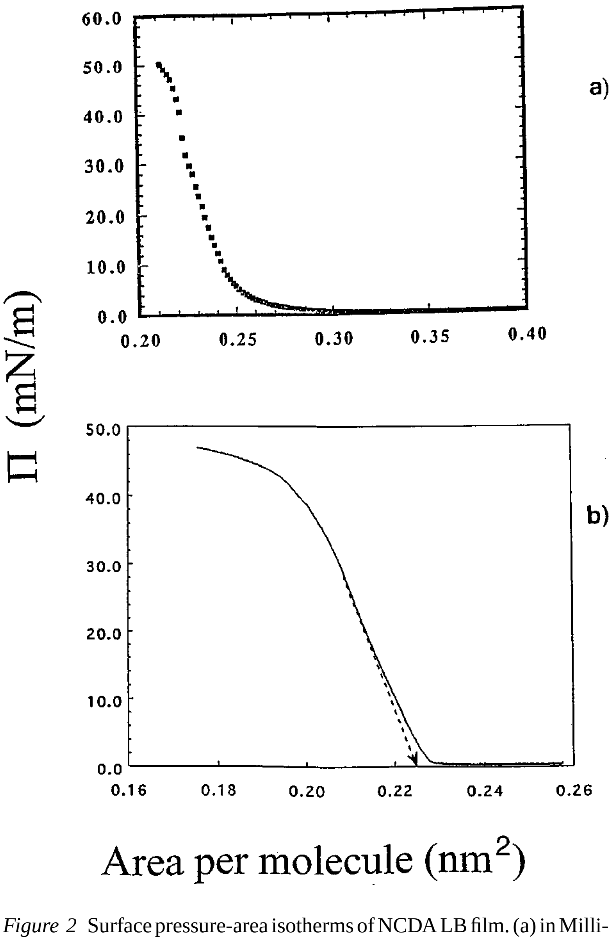

Figure 2 Surface pressure-area isotherms of NCDA LB film. (a) in Milli-Q water; (b) in 1.0 mM CdCl$_2$(aq).

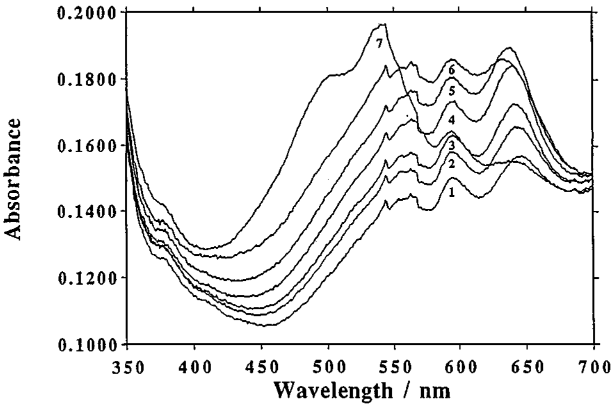

Figure 3 UV-Visible absorbance spectra of NCDA/Cd^{2+} LB film at different UV exposure times of polymerization. 1) 30 s; 2) 60 s; 3) 120 s; 4) 300 s; 5) 600 s; 6) 30 min; 7) 60 min.

The exposure of the 19 layer NCDA Langmuir-Blodgett (LB) films to UV light resulted in the polymerisation of the film. The polydiacetylene formed exhibits a rigid, one-dimensional, conjugated backbone, which results in a strong π-π^* absorption in the visible region [20]. Therefore, the NCDA LB film polymerisation was monitored by the variation of the absorbance spectra with the illumination time. An increase in the absorbance was observed creating two peaks at 640 and 600 nm resulting on the formation of a "blue" color film. After about 30 min, a decrease in the 600 and 640 nm peaks was verified with simultaneous increases in the peaks at 500 and 530–540 nm as a result of the conversion to the "red" color NCDA polymer LB film. After 60 min irradiation no further significant changes were detected in the absorbance spectra. These results are in good agreement with similar previous works where a topological model with the formation of cross-links in the organic chain was proposed for the polydiacetylenes formation process. The "blue" form replacement by the "red" form is believed to be associated with a phase transition from a monoclinic to an orthorhombic arrangement [20]. Fig. 3 shows the absorbance spectra changes with the UV illumination time. We believe we had the formation of the trans-isomer of NCDA polymer LB film because it is the most thermodynamically stable of the two forms at room temperature [21, 22]. The polymerisation of the NCDA film occurs by the 1,4 addition reaction suggested by Lopez *et al.* [23] and Tieke *et al.* [24] according to the Equation 1 shown below.

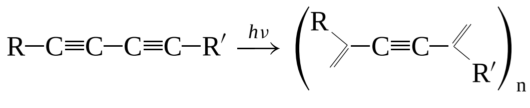

$$\mathrm{R{-}C{\equiv}C{-}C{\equiv}C{-}R'} \xrightarrow{h\nu} \left(\overset{\mathrm{R}}{\rangle}\!\!{=}\mathrm{C{\equiv}C{-}}\!\!\langle_{\mathrm{R'}} \right)_n \qquad (1)$$

3.1. Particle formation and growth

We have shown in our previous work [1, 2] that the exposure of cadmium arachidate (CdAr) LB films to H$_2$S(g) produced CdS nanoparticles and arachidic acid. The subsequent immersion of the LB film in CdCl$_2$(aq) solution regenerated 100% of the cadmium salt form (CdAr). Therefore, using the sequence gassing/immersion we were able to nucleate and grow the CdS in LB film matrix. We have assumed that the replacement of the arachidic acid by NCDA polymer film would follow similar reactions as proposed by

Equations 2 and 3:

$$\left[\mathrm{CH_3(CH_2)_{15}C{-}C{\equiv}C{-}C(CH_2)_8CO^{2-}}\right]_2\mathrm{Cd^{2+}} + \mathrm{H_2S(g)} \rightarrow \mathrm{2CH_3(CH_2)_{15}C{-}C{\equiv}C{-}C(CH_2)_8CO_2H} + \mathrm{CdS(s)} \quad (2)$$

$$\mathrm{2CH_3(CH_2)_{15}C{-}C{\equiv}C{-}C(CH_2)_8CO_2H} + \mathrm{CdCl_2(aq)} \rightarrow \left[\mathrm{CH_3(CH_2)_{15}C{-}C{\equiv}C{-}C(CH_2)_8CO^{2-}}\right]_2\mathrm{Cd^{2+}} + \mathrm{2HCl(aq)} \quad (3)$$

Using the alternating sequence of exposure of the NCDA LB film to $H_2S(g)$ followed by immersion in a $CdCl_2$ (aq) solution, permitted the construction of LB films containing CdS semiconductor particles with dimensions varying from "Q-state" to "bulk crystal" range (2–10 nm diameter). CdS particles formed on the first H_2S gassing act as "seeds" for subsequent growth when more CdS is produced in the LB film. The growth in the CdS particle size could be monitored by a "red shift" in the UV-visible absorbance spectra after each immersion/gassing cycle [25–27]. Direct measurement of particle size was also made using an atomic force microscopy (AFM) [2].

Fig. 4a and b show the absorbance spectra of CdS nanoparticles formation and growth in unpolymerized and polymerized NCDA LB films, respectively. The XPS results have confirmed the formation of CdS particles in the proportional ratio Cd/S: 1:1.1, in the polymerized LB film. Based on the fact that each Cd^{2+} is bound to 2 NCDA organic chains we were able to estimate average concentration of species in the LB film. These results are shown in Table I. There was no significant difference between the polymerized and unpolymerized film regarding to the formation and growth of CdS "Q-state" particles in the LB film matrix. This fact was expected because of the LB film method almost always presents an ordered and compact structure that would itself restrain the size of particles formed in the matrix, minimizing any possible effect of the polymerized film. Both spectra (Fig. 4a and b) have shown similar values of absorption onset of 420 ± 10 nm for the CdS nanoparticles formation ($E = 3.12 \pm 0.07$ eV), corresponding to 2–3 nm average particle diameter. After a sequence of 5 gassing/immersion cycles we have found CdS particles with average size of 8 nm (510 ± 10 nm) indicating they have reached the crystalline ("bulk") dimensions.

TABLE I XPS analysis results of NCDA polymer LB film after exposure to H_2S (g) for CdS nanoparticles formation

Element	Sample A (%)	Sample B (%)	Theoretical value	Average X
Cd	0.9	1.1	—	1.0
S	0.9	0.9	—	0.9
C	86.2	88.0	—	87.1
Cd/S (Ratio)	1.0:1	1.2:1	1:1	1:1.1

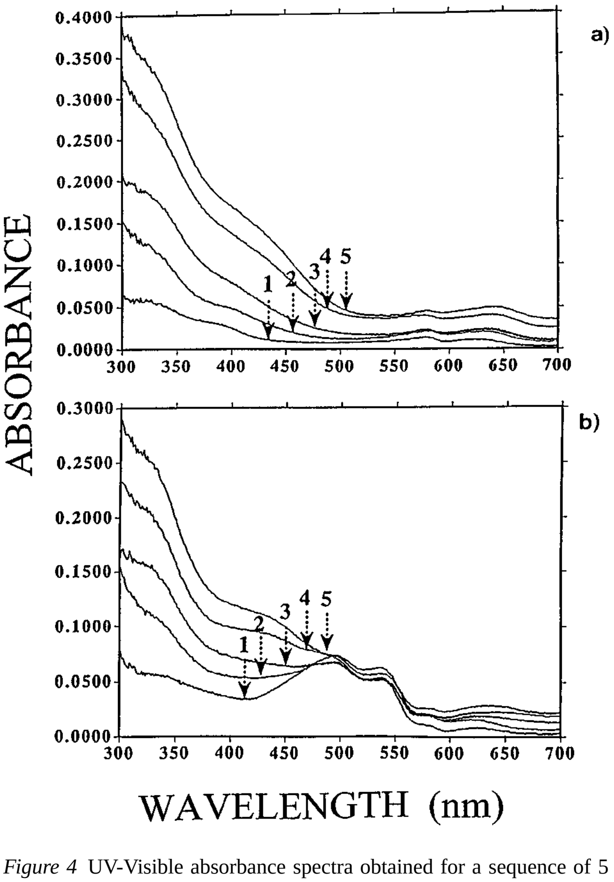

Figure 4 UV-Visible absorbance spectra obtained for a sequence of 5 gassing/immersion of a 19-layer NCDA/Cd^{2+} LB film deposited onto ITO-glass. (a) Unpolymerized NCDA LB film. (b) Polymerized NCDA LB film 60 min in UV light.

3.2. PEC cell results

The photoelectrical system based on a semiconductor/liquid junction has been studied in a number of previous works [2, 3, 28–30]. The main reaction steps are believed to be,

$$\mathrm{CdS} + \mathrm{h^+} \rightarrow \mathrm{CdS(h^+/e^-)} \quad (4)$$

$$\mathrm{SO_3^{2-}(aq)} + 2\mathrm{h^+} + \mathrm{H_2O} \rightarrow \mathrm{SO_4^{2-}(aq)} + 2\mathrm{H^+(aq)} \quad (5)$$

$$2\mathrm{SO_3^{2-}(aq)} + 2\mathrm{h^+} \rightarrow \mathrm{S_2O_6^{2-}(aq)} \quad (6)$$

It should be noted that the electron, from the electron-hole pair generated in reaction (4), must percolate through the LB film before reaching the ITO conductive layer. The efficiency of this step will directly affect the electron current flow.

The photoresponse of the cell was examined via an applied polarisation cycle with a bias varying from 0 to −1000 mV/SCE. The energy conversion from the incident light to electrical power was calculated by the difference in the area of the I-V curves for the "dark" and "light" conditions. The open-circuit voltage V_{OC} for a 19 layers LB film with 10 nm CdS particles (5 gassed/immersion cycles) was −800 to −900 mV (SCE), and the fill factor (FF) was up to 70% (20–25% typical). This value of the open circuit voltage (V_{OC}) of "bulk" CdS particles is comparable to that obtained by Minoura *et al.* [31] using PEC cells constructed with a single crystal CdS electrode and immersed in different concentrations of sulfur based electrolytes (SO_3^{2-}, S^{2-}, $S_2O_3^{2-}$, SO_4^{2-}). The electron-hole pair generated in the

CdS must go through the NCDA LB film, resulting in energy decay, reflected in the V_{OC} value measured by the I-V polarisation curves. It is expected to have a V_{OC} measurement lower than the theoretical maximum calculated from subtraction of the energy levels of the CdS conduction and valence bands ($V_{\mathrm{OC}}^{\max} = E_{\mathrm{CB}} - E_{\mathrm{VB}}$). It should be noted that, as the system investigated involves CdS "Q-state" particles, the energy of the electron-hole pair will be different from those "bulk" values. The photoresponse will reflect an overall contribution of several discrete energy states generated by the quantization effect in the CdS. The photoelectrochemical behaviour of the system based on the NCDA polymer LB film with CdS nanoparticles dispersed in the matrix has shown no significant difference with our previous results obtained with similar system based on arachidic acid LB film [2, 3]. At first moment one would expect to observe some improvement on the PEC system photoresponse with the replacement of the organic chain of arachidic acid by NCDA conductive polymer. This is based on the theoretical availability of unsaturated bonds with correspondent π-electrons to increase the conductivity of the NCDA compared to the arachidic film. Actually, some minor increase on the intrinsic electrical conductivity was observed but the overall contribution to the current/voltage output was not significant. These phenomena could be explained assuming a nonuniform conductive behaviour of the NCDA film as proposed by Shimanoe and Sakashita [32]. They have shown different conductivity of diacetylene films on the three coordinated axes x, y and z, where the film behaves as a dielectric in the z direction, in the plane perpendicular to the unsaturated double and triple bonds. Therefore, we can assume that the NCDA LB polymer actually acted as a dielectric barrier in our PEC system. We have also run additional experiments trying to reduce such dielectric effect on the NCDA by doping with I_2(g) as suggested in the literature [21, 22]. The XPS results have indicated the presence of I_2 incorporated to the NCDA LB film matrix and the 4-point probe have also shown an increase in the electrical of conductivity of 10^2 to 10^3 comparing to the undoped NCDA. Unfortunately, the I_2 doping have made the PEC unstable promoting the corrosion of the semiconductor CdS particles in the film, resulting on short time degradation of the photoresponse.

3.3. Photoelectrochemical response as function of particle size

Photoelectrochemical experiments with chemically-deposited and electroplated CdS and CdSe "Q-state" particles were previously reported by Hodes and Albu-Yaron [33]. They have observed a complex behaviour of the PEC cell concerning to V_{OC} values, suggesting the necessity of interpretation of individual and collective behaviour of these semiconductor "Q-state" particles.

The typical photoelectrochemical behaviour observed in our experiments for CdS nanoparticles in NCDA LB film is shown in Fig. 5. The most striking feature of the results shown in Fig. 6 is that the change in the photovoltage (plotted as the difference between V_{OC} "light" and V_{OC} "dark"), due to the increase in CdS particle size (equivalent to CdS concentration), from "Q-state" to "bulk" range, is opposite to that expected based on the increase band gap energy (hence conduction band potential) with decreasing particle size [34, 35]. It can be assumed that the photo generated hole (h^+) is almost immediately scavenged by the electrolyte solution due to the relatively high concentration of reductant (SO_3^{2-}/1.0 M) [31]. On the other hand, the photogenerated electron (e^-) must move through the high resistance hydrocarbon film to reach the conductive ITO layer to complete the electrical circuit. This process might result in an energy loss in the electron and cause a lower effective photovoltage to be measured. As the CdS particle size and molar concentration are increased, some particles may link together, forming lower resistance conduits, resulting in less energy being lost in the electron path. Different electrical resistivities are expected due to the existence of interfaces,

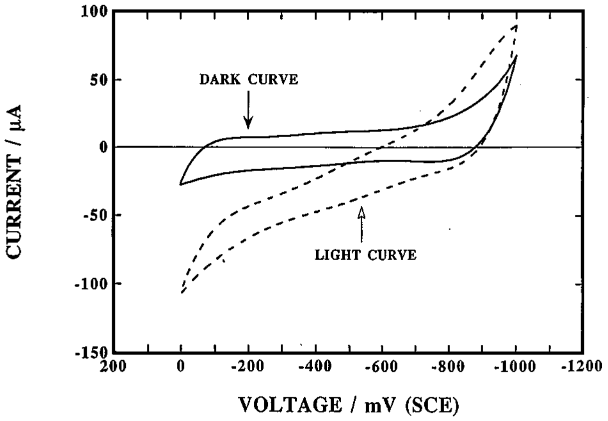

Figure 5 Typical current-voltage response curves for 19-layer $Cd(NCDA)_2$ LB film obtained from the sequence of 5 immersions in Cd^{2+}(aq) solution and exposure to H_2S(g) cycles. The polarisation curves were obtained for a scanning cycle from 0 to −1000 mV/SCE. Solid line shows "dark" photoresponse; dashed line indicates the "light" results.

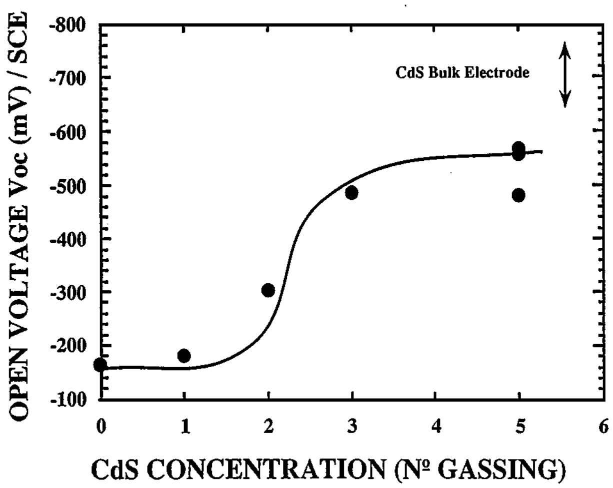

Figure 6 Open circuit voltage versus number of immersions in Cd^{2+}(aq) solution and exposure to H_2S(g) cycles for a 19-layer $Cd(NCDA)_2$ LB film obtained from illumination of 600±50 mW/m^2 from a 150 W xenon lamp.

material type and electrical contacts. A major contribution is likely to be associated with the high resistance of the LB film matrix. The resistance decreases and the conduction band potential drops with increasing particle size, the former because the particles interconnect and the latter because of the "Q-state" effect. The combined effect is measured through the V_{OC} value.

The explanation given for the variation in the observed V_{OC} values with particle size is to some extent similar to that suggested by Hodes *et al.* [36]. These authors investigated the photo response of electrodeposited and chemical deposited semiconductor particles (CdS, CdSe, PbSe) on conductive substrates (ITO, Ti). Although no organic film was present in these films, a model was proposed which focused on the differential h^+/e^- pair transport through the deposited interconnecting layer of semiconductor particles, which resulted in energy loss along the electron path to the support electrode.

4. Conclusion

An active and stable photoelectrochemical cell was constructed incorporating CdS nanoparticles in a conductive NCDA polymer LB film matrix based on an n-type semiconductor/liquid junction. It has not been noted any significant contribution of the conductive NCDA film on the overall device photoelectrical response compared to the previous arachidic acid LB film matrix.

Acknowledgements

HSM thanks the CNPq for support of a Fellowship from the Government of Brazil. We are also grateful to the ARC Advanced Mineral Products Special Research Centre for infrastructure support. The authors also thank Mr. Thomas Gengenbach for the XPS analysis.

References

1. R. S. URQUHART, D. N. FURLONG, H. S. MANSUR, F. GRIESER, K. TANAKA and Y. OKAHATA, *Langmuir* **10** (1994) 899.
2. H. S. MANSUR, F. GRIESER, M. S. MARYCHURCH, S. BIGGS, R. S. URQUHART and D. N. FURLONG, *J. Chem. Soc., Faraday Transactions* **91** (1995) 665.
3. H. S. MANSUR, F. GRIESER, R. S. URQUHART and D. N. FURLONG, *ibid.* **91** (1995) 3399.
4. H. S. MANSUR, F. GRIESER and W. L. VASCONCELOS, *Acta Microscopica* **5** (1996) 312.
5. *Idem., ibid.* **6** (1997) 256.
6. R. S. URQUHART, D. N. FURLONG, H. S. MANSUR and F. GRIESER, in 3rd Australian/Japan Symposium on Surface and Colloid Science, Fukuoka, Japan, 28–29 October 1994, p. 78.
7. F. GRIESER, H. S. MANSUR, R. S. URQUHART and D. N. FURLONG, in 3rd Australian/Japan Symposium on Surface and Colloid Science, Fukuoka, Japan, 28–29 October 1994, p. 28.
8. D. N. FURLONG, R. S. URQUHART, N. GEDDES, F. GRIESER and H. S. MANSUR, 2nd Australian/Japan Symposium on Surface and Colloid Science, Tokyo, Japan, 28–29 October 1993.
9. R. S. URQUHART, D. N. FURLONG, T. GENGENBACH, N. J. GEDDES and F. GRIESER, *Langmuir* **10** (1994) 899.
10. J. T. GRANT, *SIA Surface. Interface Anal.* **14** (1989) 271.
11. J. H. SCOFIELD, *J. Electron Spectrosc. Relat. Phenom.* **8** (1976) 129.
12. M. P. SEAH and W. A. DENCH, *SIA Surface. Interface Anal.* **1** (1979) 2.
13. L. S. MUROV, I. CARMICHAEL and G. L. HUG, Handbook of Photochemistry, 2nd Edition (Marcel Dekker, New York, 1993).
14. B. TIEKE, G. LIESER and G. WEGNER, *J. Polym. Sci. Polym. Chem. Ed.* **17** (1979) 1631.
15. B. TIEKE, V. ENKELMANN, H. KAPP, G. LIESER and G. WEGNER, *J. Macromol. Sci. Chem.* **15** (1981) 1045.
16. B. TIEKE and G. LIESER, *J. Colloid Interface Sci.* **88** (1982) 471.
17. F. R. AHMED and E. G. WILSON, *Thin Solid Films* **187** (1990) 141.
18. H. RINGSDORF and D. DAY, *J. Polym. Sci. Lett. Edn.* **16** (1978) 205.
19. M. A. COLLINS, *J. Polym. Sci. Olym. Phys.* **26** (1988) 367.
20. A. A. DECKERT, L. FALLON, L. KIERNAN, C. CASHIN, A. PERRONE and T. ENCALARDO, *Langmuir* **10** (1994) 1948.
21. H. SHIRAKAWA, E. J. LOUIS, A. G. MCDIARMID, C. K. CHIANG, Y. PARK and A. J. HEEGER, *J. Chem. Physics* **49**(11) (1978).
22. H. SHIRAKAWA, E. J. LOUIS, A. G. MCDIARMID, *et al.*, *J. C.S. Chem. Comm.* (1977).
23. E. LOPEZ, D. F. O'BRIEN and T. H. WHITESIDES, *J. Amer. Chem. Soc.* **104** (1982) 305.
24. B. TIEKE, T. SATO, T. OTSU and R. W. RICHARDS, *Advances in Polymer Sci.* (1985).
25. F. GRIESER, D. N. FURLONG, D. SCOBERG, I. ICHINOSE, N. KIMIZUKA and T. KUNITAKE, *J. Chem. Soc. Faraday Trans.* **88** (1992) 2207.
26. D. J. SCOBERG, F. GRIESER and D. N. FURLONG, *J. Chem. Soc. Chem. Commun.* (1991) 515.
27. Y. WANG and N. HERRON, *Phys. Rev. B* **42** (1990) 7253.
28. D. HAYES, P. A. FREEMAN, P. MULVANEY, F. GRIESER, T. W. HEALY and D. N. FURLONG, *Ber. Bunsenges. Phys. Chem.* **91** (1987) 231.
29. M. GUTIERREZ and A. HENGLEIN, *Ber. Bunsenges. Phys. Chem.* **87** (1983) 474.
30. A. HELLER and B. MILLER, *Electrochimica Acta* **25** (1980) 29.
31. H. MINOURA and M. TSUIKI, *ibid.* **23** (1978) 1377.
32. K. SHIMANOE and M. SAKASHITA, *Jpn. J. Appl. Phys.* **32** (1993) 1064.
33. G. HODES and A. ALBU-YARON, *Proc. Electrochem. Soc.* **88** (1988) 298.
34. M. GRÄTZEL, Heterogeneous Photochemical Electron Transfer (CRC Press, Florida, 1989).
35. R. VOGEL, H. POHL and H. WELLER, *Chem. Phys. Letter* **174** (1990) 241.
36. G. HODES, I. D. J. HOWELL and L. M. PETER, *J. Electrochem. Soc.* **139** (1992) 3136.

Received 27 July 1998
and accepted 4 May 1999